The electronic structure of some monovalent-metal intercalates of TiS_2

1989 J. Phys.: Condens. Matter 1 4297

(http://iopscience.iop.org/0953-8984/1/27/003)

J. Phys.: Condens. Matter 1 (1989) 4297–4309. Printed in the UK

The electronic structure of some monovalent-metal intercalates of TiS_2

J Dijkstra†, C F van Bruggen and C Haas
Laboratory of Inorganic Chemistry, Materials Science Centre of the University, Nijenborgh 16, 9747 AG Groningen, The Netherlands

Received 2 September 1988, in final form 3 January 1989

Abstract. The electronic structures of the layered compound TiS_2 and its intercalates $LiTiS_2$, $NaTiS_2$ and $AgTiS_2$ are calculated using the ASW method. Various deviations from the rigid-band model are observed, of which the increase of the Ti-3d/S-3p gap and the variation of the inter-sandwich and intra-sandwich interactions between S-3p orbitals are the most pronounced. The effect of the flattening of the TiS_2 slabs—such as occurs at the 3R(I)–3R(II) transition in Na_xTiS_2 for $x \simeq 0.7$—on the electronic structure is calculated for Na_1TiS_2 and is shown to be coupled with an increased ionicity in the Ti–S bond.

1. Introduction

Various guest atoms—for example alkalis (Whittingham 1978, Rouxel 1979), silver (Gerards *et al* 1984/1985) and first-row transition metals (Inoue *et al* 1985, Negishi *et al* 1987, Yamasaki *et al* 1987)—can be inserted in the van der Waals gap. Metals intercalated in TiS_2 have in common that they donate electrons into the narrow lowest-lying Ti-3d band. While for the host compound TiS_2 there has been for many years a standing discussion about its semiconducting/semimetallic character, the above-mentioned intercalates all show metallic conductivity (Bouwmeester 1988, Gerards 1987, Koyano *et al* 1986, 1987).

The electronic structure of intercalates is usually described by a rigid-band model: one assumes that the TiS_2 band structure is unchanged during intercalation and that only the Fermi level is shifted to a higher energy, since there is an electron transfer from the intercalant atoms to the host lattice. That this model is an oversimplification was shown by McCanny (1979) and Umrigar *et al* (1982), who performed band-structure calculations on $LiTiS_2$.

Structural parameters of the alkali metal intercalates of TiS_2 were obtained by Rouxel and co-workers (Rouxel 1979). The most remarkable feature is the occurrence of two different coordinations of alkali atoms by S: (trigonally distorted) octahedral and trigonal-prismatic coordination. On the basis of an 'ionicity–structure diagram', Rouxel (1976, 1979) predicted the coordination of the alkali atom. The parameters used are the size of the alkali (1+) ion r_{A+}, the concentration of intercalated atoms x and the ionicity of the host-lattice T–S bond f_i. From this diagram it is found that increasing r_{A+} and decreasing x and f_i favour the trigonal-prismatic coordination. A similar partitioning in

† Present address: Philips Research Laboratories, Eindhoven, The Netherlands.

0953-8984/89/274297 + 13 $02.50

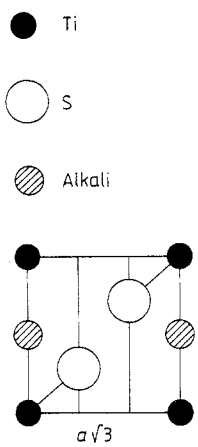

Figure 1. The (110) cross section of the hexagonal unit cell of 1T-TiS_2.

different coordinations as a function of inter-atomic distances is described by Hibma (1982). The trend wherein octahedral coordination occurs for strongly ionic compounds, while trigonal-prismatic coordination is observed with more covalent materials is in accordance with the results of cluster calculations (Huisman *et al* 1971).

In Rouxel's considerations it is assumed that the host sandwiches have a constant effect throughout the series. However, in some cases the TiS_2 sandwiches themselves change appreciably during intercalation. The most remarkable example is found in the Na_xTiS_2 system. In this system there are two first-stage compounds (Molinie *et al* 1984, Hibma 1980), 3R(I) ($0.40 < x < 0.64$, Na trigonal-prismatically coordinated by S) and 3R(II) ($0.75 < x < 1.0$, Na octahedrally coordinated). When passing from the 3R(I) to the 3R(II) phase the dimension in the c direction is reduced, while that in the a direction is increased, so the unit-cell volume remains about the same. A similar effect is observed in the Na_xVS_2 and Na_xVSe_2 systems (Wiegers 1980, Van Bruggen 1982).

To study the effect of intercalation in general and the effect of the change in lattice parameters of the host compound in particular, we have performed band-structure calculations for TiS_2 and $LiTiS_2$, two modifications of $NaTiS_2$ and $AgTiS_2$. Our calculated electronic structure for $LiTiS_2$ is in agreement with the LAPW results of Umrigar *et al* (1982). For $NaTiS_2$ we come to conclusions different from those reported by Whangbo *et al* (1985).

2. Crystal structure and computational details

TiS_2 crystallises in the 1T-type CdI_2 structure (space group D^3_{3d} or $P\bar{3}m1$; see figure 1): one Ti at (0, 0, 0) and two S at $(\frac{1}{3}, \frac{2}{3}, z)$ and $(\frac{2}{3}, \frac{1}{3}, -z)$ with $z = \frac{1}{4}$ (Chianelli *et al* 1975). The cell parameters are given in table 1. The c/a ratio is slightly larger than the ideal value. The value of z, 0.250, indicates that the inter-sandwich and intra-sandwich separations between S layers are equal.

Li intercalated in TiS_2 occupies the octahedral sites in the van der Waals gap. $LiTiS_2$ has the same space group as its host compound, with the Li atoms at $(0, 0, \frac{1}{2})$ (Dahn *et al* (1980); see figure 1). The unit-cell volume is 11.5% larger than that of TiS_2, which is

Table 1. Crystal structure parameters and Wigner–Seitz sphere radii used in the band-structure calculations. The lattice constants are a and c, $2z_S c$ is the intra-sandwich distance between S layers, d(Ti–S) the Ti–S distance, (c/a)(Ti) the c/a ratio of the trigonal anti-prism of S around Ti (ideal value: 1.633/2), and V_{cell} the unit-cell volume. r_{Ti}, r_S and r_A are the Wigner–Seitz radii of Ti, S and the alkali (or empty sphere in TiS_2).

	TiS_2	$LiTiS_2$	$NaTiS_2$(I)	$NaTiS_2$(II)
a (Å)	3.412	3.455	3.455	3.550
c (Å)	5.695	6.195	7.030	6.660
c/a	1.6691	1.7931	2.035	1.876
V_{cell} (Å^3)	57.417	64.044	72.688	72.688
z_S	0.250	0.232	0.205	0.195
d(Ti–S) (Å)	2.431	2.459	2.460	2.427
(c/a)(Ti)	1.669/2	1.664/2	1.667/2	1.465/2
r_{Ti} (Å)	1.058	1.058	1.058	1.058
r_S (Å)	1.782	1.831	1.831	1.831
r_A (Å)	1.058	1.217	1.569	1.569

almost completely due to the increase in the c parameter (see table 1). The change in the z parameter indicates that the TiS_2 sandwich is itself hardly changed.

In the Na_xTiS_2 system two different crystal structures occur, depending on the Na concentration. In both structures the stacking of the TiS_2 slabs is changed as compared with that in TiS_2 and $LiTiS_2$, while the unit cell is tripled in the c direction. In the 3R(I) structure Na is trigonal-prismatically coordinated by S. The existence range of the 3R(I) modification is $0.40 < x_{Na} < 0.64$. Octahedrally coordinated Na is found in the 3R(II) phase for Na concentrations $0.75 < x_{Na} < 1.0$. Molinie *et al* (1984) found by x-ray diffraction that at the transition from the 3R(I) to the 3R(II) phase the c parameter is reduced from 7.03 to 6.66 Å, while the a parameter increases from 3.45 to 3.55 Å, which leaves the unit-cell volume almost unchanged.

Self-consistent band-structure calculations of TiS_2 and some of its monovalent metal intercalates were performed using the augmented-spherical-wave (ASW) method (Williams *et al* 1979). The local-density approximation, as given by Hedin and Lundqvist (1971), was used to include the effects of exchange and correlation. Scalar relativistic effects (mass velocity and Darwin terms (Methfessel and Kübler 1982)) were included. In the ASW method the crystal is subdivided into Wigner–Seitz spheres surrounding each atom. The potential is taken to be spherically symmetric within each sphere. The radii of the Wigner–Seitz spheres should be chosen in such a way that the sum of the volumes of the overlapping spheres is equal to the unit-cell volume. Therefore the radii depend on the unit-cell dimensions. Generally the best filling of the crystal volume by Wigner–Seitz spheres is obtained when the overlap between neighbouring spheres is minimised; in that case the space that is not within any one of the spheres is also minimised. Because the main object of our calculations is a comparison of the intercalation compounds $LiTiS_2$, $NaTiS_2$(I) and $NaTiS_2$(II), the same radii for Ti and S were chosen for these compounds. The radii for the intercalated alkali atoms are then determined from the unit-cell volume. For TiS_2 the same value of r_{Ti} and a slightly smaller value of r_S were used. The effect of the small difference in r_S on the electronic structure is small. For the host compound TiS_2 we have included a sphere with zero nuclear charge on the octahedral site in the van der Waals gap. As basis functions we used the 4s, 4p and 3d

functions for Ti, the 3s, 3p and 3d functions for S and the *n*s and *n*p functions for the alkali atom and the empty sphere. The Wigner–Seitz radii are given in table 1.

3. Results and discussion

3.1. TiS_2

The calculated energy bands along the high-symmetry lines in the Brillouin zone and the density of states of 1T-TiS_2 are plotted in figure 2. The two lowest-lying bands are mainly composed of S 3s states. Between -5 eV and the Fermi level E_F are six bands of S 3p origin. The top and bottom of this set of bands are situated at Γ. Just above E_F we find five Ti 3d bands, in which the crystal-field splitting of an octahedrally coordinated Ti atom (three lower-lying non-bonding t_{2g} and two anti-bonding e_g states) is easily recognised. From the partial densities of states it is evident that the Ti–S bonding is not strictly ionic, and that there is strong covalent mixing, especially between Ti e_g and S 3p states.

In this calculation we find a very small indirect overlap of 0.007 eV between the top of the S 3p valence band at Γ and the bottom of the Ti 3d conduction band, situated at L. The direct gap at Γ is 0.45 eV. After much discussion, experimentalists seem to have agreed on TiS_2 being a semiconductor with an indirect band gap of 0.2–0.3 eV on the basis of magnetic and transport data (Wilson 1977) and angle-resolved photoemission (Barry *et al* 1983). Since 1972 more than ten calculated band structures of TiS_2 have been published. A compilation of these calculations is included in the Review Article on the electronic structures of layered compounds by Doni and Girlanda (1986). The major difference between the various calculations concerns the S-3p/Ti-3d gap. Doni and Girlanda conclude that the results of the self-consistent general potential LCAO calculations by Zunger and Freeman (1977) are in closest agreement with experiment, although no relativistic effects were included. In our calculation, scalar relativistic effects are included. However, we use muffin-tin potentials and it is well known that this spherical approximation of the potential tends to decrease the p/d gap (Mattheiss 1973). Coehoorn *et al* (1985) tried to overcome this difficulty, which is partly due to polarisation effects, by shifting the chalcogen atoms somewhat towards the transition-metal atoms by reducing the *z* parameter of the chalcogens to a rather large extent. However, in the case of ASW calculations with empty spheres on the octahedral sites in the van der Waals gap a smaller shift—about 50% smaller than that calculated by Coehoorn *et al* (1985)—of the chalcogen atoms is necessary for obtaining a proper description of the angle-resolved photoemission results (Dijkstra 1987).

Our calculated p/d gap of -0.007 eV is 0.2 to 0.3 eV too small, probably because of the use of muffin-tin potentials. It is, however, in better agreement with experiment than the results of scalar relativistic LAPW calculations, where a p/d overlap of -0.5 eV is found (Umrigar *et al* 1982).

3.2. $LiTiS_2$

McCanny (1979) was the first to make a comparative analysis of pure TiS_2 and lithium-intercalated TiS_2, using a semi-empirical tight-binding method. An LAPW study of the same system was performed by Umrigar *et al* (1982). Their results are in qualitative agreement—only the position of the Li 2s band is rather different: using the tight-binding

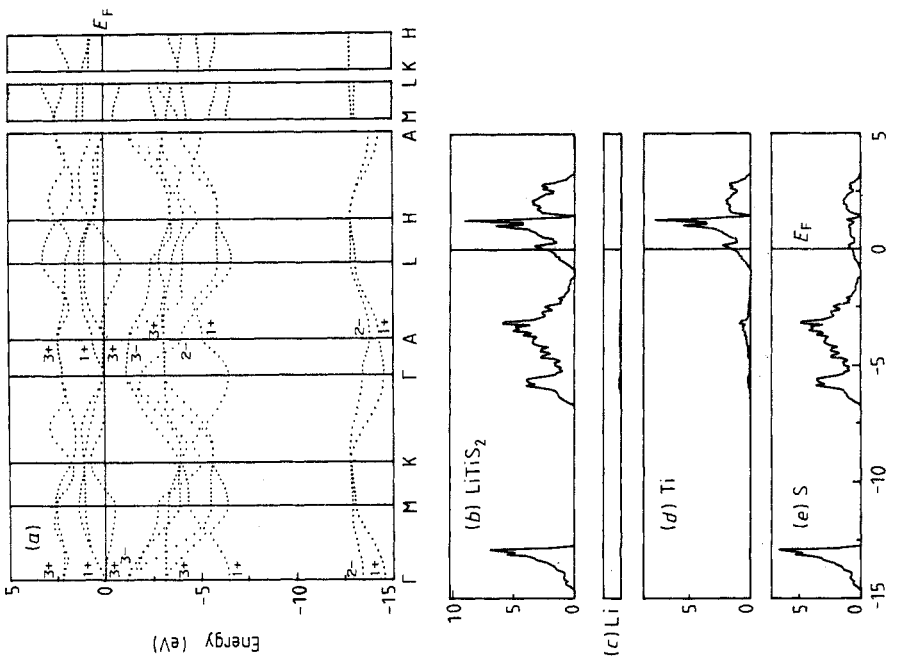

Figure 3. The band structure (*a*) and the total (*b*) and partial ((*c*)–(*e*)) DOS of $LiTiS_2$. DOS units: states eV^{-1}/formula unit.

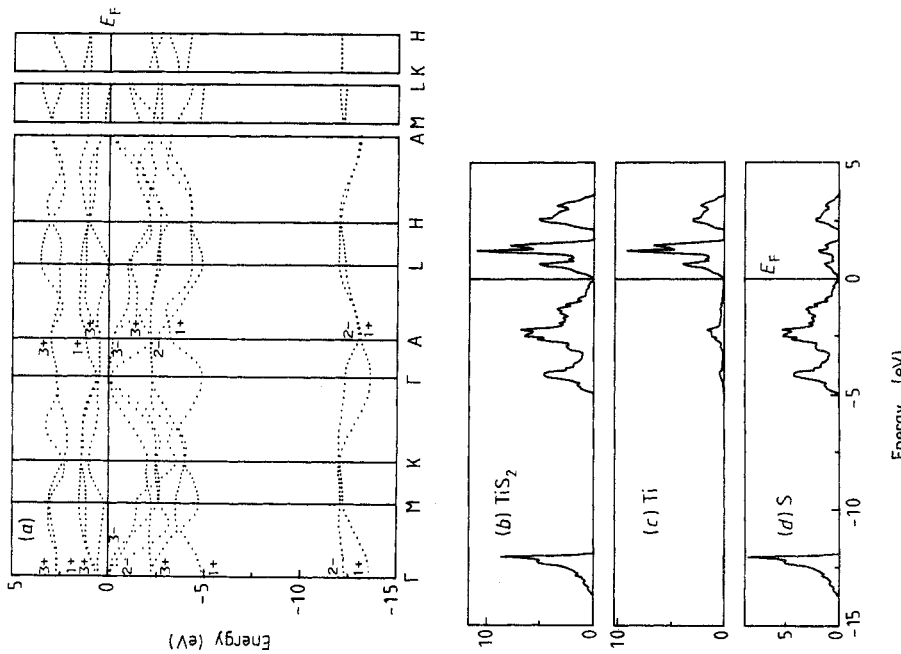

Figure 2. The band structure (*a*) and the total (*b*) and partial ((*c*)–(*d*)) DOS of TiS_2. DOS units: states eV^{-1}/formula unit.

Table 2. The band width W (in eV), energy gap (in eV) and DOS at the Fermi level $N(E_F)$ (in states eV^{-1}/formula unit).

	TiS_2	$LiTiS_2$	$NaTiS_2$(I)	$NaTiS_2$(II)
W(S 3p)	4.94	5.53	5.22	5.02
W(Ti t_{2g})	1.61	2.27	2.09	1.79
W(Ti e_g)	1.50	1.61	1.64	1.27
d/p gap	−0.007	+0.23	+0.49	+1.09
d/p gap at Γ	+0.45	+1.12	+1.20	+1.58
$N(E_F)$	0.002	2.63	2.77	3.81

method the Li 2s band intersects the Ti 3d states, while in the LAPW calculation its position is well above these states. Both sets of authors found that the rigid-band model is a reasonable first-order approximation. The deviations from the rigid-band model are: (i) the d/p gap increases by ≈0.7 eV; (ii) bands with S $3p_z$ character become less dispersive in the ΓA direction; (iii) the Ti e_g–t_{2g} splitting decreases by ≈0.3 eV.

The energy bands and densities of states from our calculation on $LiTiS_2$ are shown in figure 3 and the parameters used are given in table 1. In table 2 some characteristic values of the calcuated electronic structures of TiS_2 and its Li (and Na) intercalates are listed. On comparing our results with those obtained by Umrigar *et al* (1982), agreement on the three above-mentioned deviations from the rigid-band model is found. However, in our calculations, the indirect Ti-3d/S-3p gap increases in $LiTiS_2$ by only 0.24 eV, mainly due to the widening of the lowest conduction bands. This difference between the ASW and LAPW results can be traced back to the different d/p gap found for TiS_2, while the calculated band structures for $LiTiS_2$ look very much alike. In $LiTiS_2$ the charge density around Ti is more or less spherically symmetric, while in TiS_2 it shows significant angular polarisation (Umrigar *et al* 1982). This polarisation gives rise to a difference between the results for TiS_2 calculated by the ASW and LAPW methods, since different muffin-tin sphere radii are used. Differences between distinct intercalates, however, can be accurately calculated within a muffin-tin approximation, because polarisation effects play only a minor role when the van der Waals gap is filled.

Recently, some experimental data on the physical properties of lithium-intercalated TiS_2 have been published. Resistivity and Hall effect data could be interpreted satisfactorily using the rigid-band model (Klipstein and Friend 1987, Onuki *et al* 1982). Magnetic measurements showed Pauli paramagnetic behaviour (Ahmad *et al* 1987), stongly enhanced by the correlation between the conduction electrons. This exchange enhancement of the susceptibility makes it impossible to derive a value of the density of states at the Fermi level $N(E_F)$ from the magnetic measurements.

3.3. $NaTiS_2$

In the system Na_2TiS_2 two stage-1 intercalates are found. The most striking difference between the 3R(I) and the 3R(II) structures is—besides the different coordination of the Na atoms—the compression of the TiS_2 sandwich dimension in the c direction, while that in the a direction increases. This flattening of the slabs is clearly reflected in the c/a ratio of the trigonal anti-prism of S around Ti (see (c/a)(Ti) in table 1). Because it is our aim to study the changes in the electronic structure caused by the flattening of the TiS_2 slab we have performed band-structure calculations for two imaginary structures

of Na_1TiS_2, with cell parameters as given in table 1. In order to make a valid comparison of the two calculations on $NaTiS_2$ possible, we have chosen the same unit-cell volume and Wigner–Seitz radii (see table 1) for both cases. For both calculations we have used the $LiTiS_2$ structure, i.e. octahedral coordination of the alkali atom and only one slab per unit cell. The cell axes and values of z, however, are chosen in such a way that the intra-sandwich and inter-sandwich distances are the same as in the real 3R(I) and 3R(II) phases.

We are aware that in this approximation we neglect the change in stacking of the slabs and the different coordinations of Na. Also the effects of changing the Na concentration (the 3R(I) structure is found for $x < 0.64$ and the 3R(II) structure for $x > 0.75$) are not taken into account. However, these differences are accounted for qualitatively by Rouxel's model (Rouxel 1979)—increasing x leads to a stronger ionicity, favouring octahedral coordination—but in that model no explanation is given of the compression of the TiS_2 sandwich in the c direction. Here we study the relation between the flattening of the slabs and the electronic structure.

The density of states and energy bands of $NaTiS_2$(I) and $NaTiS_2$(II) are plotted in figures 4 and 5.

The TiS_2 sandwiches are almost identical in $LiTiS_2$ and $NaTiS_2$(I). The difference in length along the c axis is caused entirely by the elongation of the inter-sandwich distance due to Na having a larger ionic radius.

Pronounced differences between $NaTiS_2$(I) and $LiTiS_2$ are found in the bands that have strong S $3p_z$ character (see table 3). The 1+ and 2− states in Γ and A give information about the inter-sandwich and intra-sandwich S-3p/S-3p interactions. The Γ_{1+} and A_{1+} (Γ_{2-} and A_{2-}) states have bonding (anti-bonding) character *within* the sandwich. *Between successive* sandwiches Γ_{1+} and A_{2-} are bonding, while Γ_{2-} and A_{1+} are anti-bonding. The energy difference ΔE_{intra} between the centres of mass of Γ_{1+}/A_{1+} and Γ_{2-}/A_{2-} is thus a measure of the intra-sandwich interaction, while the dispersion of the 1+ and 2− bands between Γ and A, $\Delta E_{\text{inter}}(1+/2-)$, is a measure of the inter-sandwich interaction. Since the intra-sandwich interaction is larger than the inter-sandwich interaction (see table 3) the order in energy is: $\Gamma_{1+} < A_{1+} < A_{2-} < \Gamma_{2-}$. The dispersions of the 1+/2− bands along ΓA, i.e. $\Delta E_{\text{inter}}(1+/2-)$, indicate that the inter-sandwich interaction decreases strongly with increasing inter-sandwich distance. There is an increased intra-sandwich interaction in the intercalates as compared with TiS_2. The c axis contraction of $NaTiS_2$(II) is reflected in the intra-sandwich interaction being larger than that found in $NaTiS_2$(I). Since all these S $3p_z$ bands involved are filled, no net bonding results.

Table 3. The characteristic energy $\Delta E_{\text{intra}}(1+/2-)$ for intra-sandwich bonding, which is equal to the energy difference between the centres of mass of the 1+ and 2− states along ΓA. The energy for inter-sandwich bonding ΔE_{inter} is equal to the mean value of the dispersion of these states along ΓA. The distance between two layers of S in a TiS_2 sandwich is d_{intra}; the distance between two layers of S across the van der Waals gap is d_{inter}.

	TiS_2	$LiTiS_2$	$NaTiS_2$(I)	$NaTiS_2$(II)
ΔE_{intra} (1+/2−) (eV)	2.73	2.86	2.84	3.00
ΔE_{inter} (eV)	2.04	1.76	0.74	0.99
d_{inter} (Å)	2.85	3.32	4.15	4.07
d_{intra} (Å)	2.85	2.87	2.88	2.58

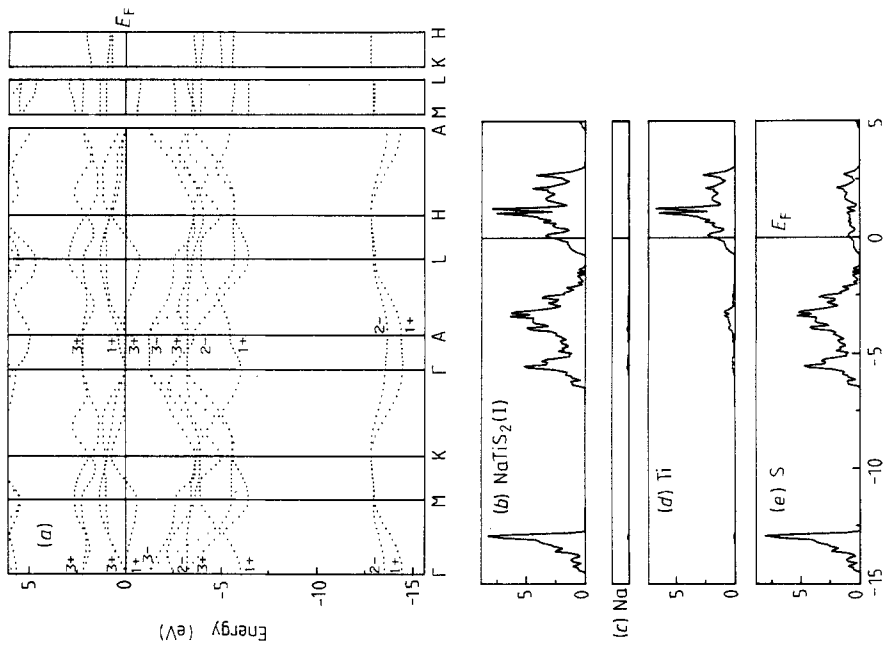

Figure 5. The band structure (*a*) and the total (*b*) and partial ((*c*)–(*e*)) DOS of $NaTiS_2$(II). DOS units: states eV^{-1}/formula unit.

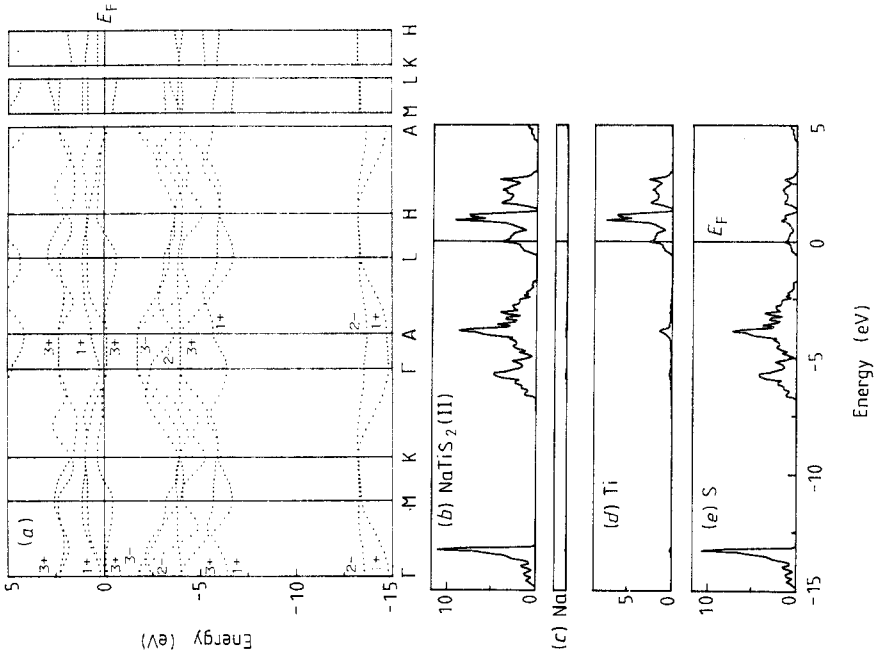

Figure 4. The band structure (*a*) and the total (*b*) and partial ((*c*)–(*e*)) DOS of $NaTiS_2$(I). DOS units: states eV^{-1}/formula unit.

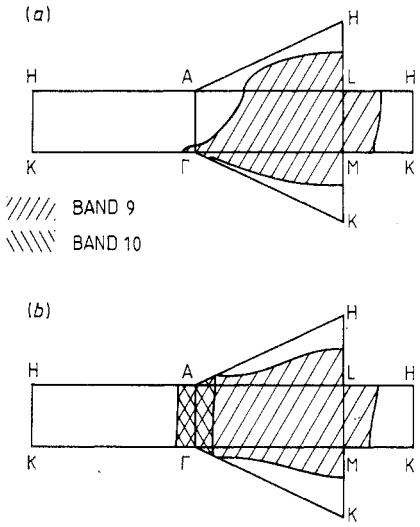

Figure 6. The Fermi surfaces of (*a*) $NaTiS_2$(I) and (*b*) $NaTiS_2$(II).

The following differences between the electronic structures of $NaTiS_2$(I) and $NaTiS_2$(II) are observed:

(i) The indirect Ti-3d/S-3p gap increases by 0.6 eV (the direct gap at Γ by 0.38 eV).

(ii) The S 3p and Ti t_{2g} and e_g band widths decrease by 0.20, 0.30 and 0.37 eV, respectively.

(iii) The density of states at the Fermi level $N(E_F)$ becomes larger (3.81 in II, compared with 2.77 states eV^{-1}/formula unit in I).

(iv) The Γ_{3+}–A_{3+} band, composed of S $3p_xp_y$ states mixed with Ti e_g, has a lower energy in II (3.20 eV in (I) and 3.82 eV in (II) below the lowest Ti Γ_{3+} state).

(v) The crystal-field splitting increases by 6% (in Γ from 2.23 eV to 2.36 eV).

(vi) The Γ_{3+}–Γ_{1+} splitting of the Ti t_{2g} states, due to the trigonal distortion of the S octahedron around Ti, changes sign and the Γ_{3+} state sinks below E_F.

(vii) As a consequence of the above-mentioned effects the Fermi surface changes considerably and an extra electron sheet is formed (see figure 6).

The changes (i), (ii), (iv) and (v) correspond to the ionicity of the Ti–S bond being larger in $NaTiS_2$(II) than in $NaTiS_2$(I). The narrowing of the Ti 3d bands and the concomitant increase of $N(E_F)$ is due to the in-plane Ti–Ti distance being larger and to the increased ionicity. One has to keep in mind that the increase in the ionicity occurring as a consequence of the flattening of the TiS_2 sandwich, calculated here, has to be superposed on the increasing ionicity responsible for the change in stacking of the slabs, as described by Rouxel (1979). The Γ_{3+}–Γ_{1+} splitting of the Ti t_{2g} band mainly results from the trigonal distortion of the S octahedron around Ti, which is rather large in the case of $NaTiS_2$(II). The c/a ratio of the octahedron around Ti in $NaTiS_2$(II) is 1.465/2 (see table 1), while the ideal value is 1.633/2.

Our band structures are not in agreement with the Ti t_{2g} dispersions calculated by a single-slab tight-binding method (Whangbo *et al* 1985), where for instance in the 3R(II) structure the bottom of the Ti 3d band is situated at Γ and no longer at L. Also the widths of the Ti 3d (t_{2g}) band in the 3R(I) and the 3R(II) structures are larger by factors of 1.6 and 2.0, respectively, than the widths calculated by us. Hence the interpretation by

Whangbo of the differences between the 3R(I) and 3R(II) structures is very questionable.

The Fermi surface of $NaTiS_2$(I) (figure 6(*a*)) consists of one electron sheet and is quite similar to that of isoelectronic 1T-VSe_2 (Myron 1980) and 1T-$TaSe_2$ (Myron and Freeman 1975) with the centre of the zone Γ occupied by electrons. When x_{Na} is smaller than 1 the region around Γ becomes unoccupied and the Fermi surface will consist of parallel cylindrically shaped rods oriented in the *c* direction, centred around ML. The Fermi surface of $LiTiS_2$ is essentially identical to that of $NaTiS_2$(I). In $NaTiS_2$(II) the twofold-degenerate Γ_{3+} and A_{3+} bands are situated below E_F, so the Fermi surface consists of two sheets (figure 6(*b*)). Since ΓM is completely occupied and little variation is found in the *c* direction, the first sheet consists of triangular rosette-shaped infinitely long cylinders oriented in the *c* direction, which are hole-like. The second electron-like sheet consists of infinitely long cylinders aligned in the *c* direction with small radii, centred around ΓA.

Only a few studies of the electronic properties of Na_xTiS_2 have been performed. Magnetic susceptibility measurements (Bouwmeester 1988) show Pauli paramagnetic behaviour of the conduction electrons but, due to the strong exchange enhancement of the susceptibility, $N(E_F)$ cannot be deduced from these measurements. However, the increase in susceptibility at the 3R(I)–3R(II) transition indicates an abrupt increase in the density of states at E_F, in agreement with our calculation. The Na Knight shift in Na_xTiS_2 also shows an abrupt increase at the 3R(I)–3R(II) transition (Molinie *et al* 1984), indicating an increase of $N(E_F)$, but a quantitative comparison between experiment and calculation is hampered by the fact that the calculation is only for $x_{Na} = 1$.

Bouwmeester (1988) also carried out transport measurements, but unfortunately only on the very similar Na_xTiSe_2 system. In Na_xTiSe_2 a 3R(I)–3R(II) transition as the sodium concentration *x* is varied is also observed and the magnetic properties of the Na_xTiS_2 and Na_xTiSe_2 systems look very much alike (Bouwmeester 1988). Hall effect and resistivity measurements by Bouwmeester show that Na_xTiSe_2 is metallic over the whole composition range. The Hall coefficient of the 3R(I) phase gives a conduction electron concentration of one electron per intercalated Na, in accordance with the single-sheet Fermi surface (figure 6(*a*)). For Na_1TiSe_2 in the 3R(II) phase a significantly lower electron concentration is found. This can be explained by the shape of the Fermi surface, which consists of electron and hole pockets (figure 6(*b*)), giving partial compensation for the Hall coefficient.

3.4. $AgTiS_2$

In Ag_xTiS_2 the maximum silver concentration is $x = 0.42$. Ag atoms are octahedrally coordinated with S (Gerards *et al* 1984/1985). To get some insight into the difference between Ag intercalates on one side and alkali intercalates on the other, the electronic structure of hypothetic fully intercalated Ag_1TiS_2 in the $LiTiS_2$ structure is also calculated. The lattice parameters used are those of $Ag_{0.42}TiS_2$ (Gerards *et al* 1984/1985): ($a = 3.429$ Å, $c = 6.400$ Å, $z_S = 0.223$. The Wigner–Seitz sphere radii $r_{Ti} = 1.164$ Å, $r_S = 1.693$ Å and $r_{Ag} = 1.622$ Å were chosen.

The most striking aspect in the results (figure 7) is the Ag 4d band, which is strongly mixed and energetically overlapping with the S 3p bands. The Ag 5s band is well above E_F, but is closer to it than the alkali s bands. The top of the S 3p band is shifted from Γ to A, where it consists of an about equal mixture of S 3p and Ag 4d states. The Ti-3d/S-

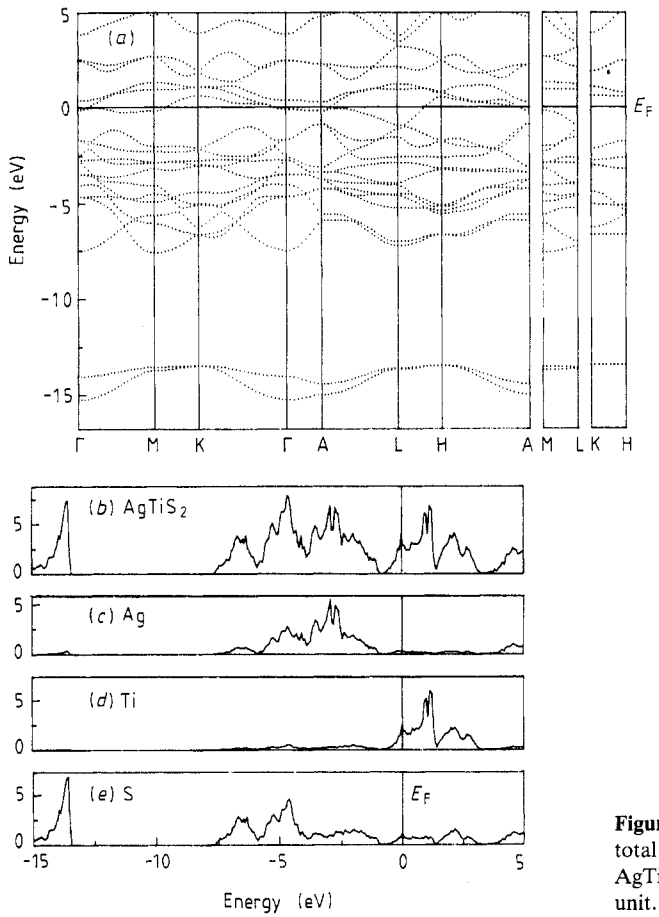

Figure 7. The band structure (*a*) and the total (*b*) and partial ((*c*)–(*e*)) DOS of $AgTiS_2$. DOS units: states eV^{-1}/formula unit.

3p gap has disappeared. The Ag-4d/Ti-3d interaction is small (see figure 7(*b*), (*c*)). The dispersion of the lowest conduction band in the *z* direction is substantial (compare M and L in figure 7(*a*)). The fact that it is impossible to intercalate more than $x_{Ag} = 0.42$ in TiS_2 (rather than 1.0 as in the case of the alkalis) may have the following cause. The Ag-4d/S-3p interaction is strong and shifts the S 3p states in $AgTiS_2$ to lower energies, but no energy is gained, since all states involved are occupied. The Ti-3d/S-3p interaction is thus diminished due to a larger energy separation. In other words, the covalent Ti–S bond is weakened by intercalating Ag. Notice that this argument is only valid because of the small Ag/Ti interaction. The weakening of the Ti–S interaction due to Ag intercalation should lead to an elongation of the Ti–S bond length. An expanded Ti–S distance is indeed found in stage II $Ag_{0.18}TiS_2$ for the Ti–S bonds adjacent to the Ag layers (Mori *et al* 1982).

The structure and the electrochemical properties of Ag_xTiS_2 as a function of *x* were studied by Gerards *et al* (1984/1985). $Ag_{0.35}TiS_2$ shows a second-order phase transition at 298.0 K from an $a\sqrt{3} \times a\sqrt{3} \times 2c$ superstructure (due to the ordering of Ag atoms in the van der Waals gap) to a disordered structure (Wiegers *et al* 1987). The electrical properties of Ag_xTiS_2 ($x = 0.33$) were reported by Meakin *et al* (1987). The compound is metallic, with increased occupation of the Ti 3d band occurring through charge transfer

from Ag, in agreement with our calculations. As the temperature was lowered the magnitude of the Hall coefficient decreased. This was attributed to Brillouin zone reconstruction associated with the ordered Ag superlattice below 298 K. Starnberg and Hughes (1987) reported a photoemission study of *in situ* intercalation of TiS_2 with Ag.

4. Conclusions

The change in electronic structure due to alkali metal intercalation into TiS_2 can be described only in a first approximation by a rigid-band model. The most striking deviations from this model are the increase in the Ti-3d/S-3p gap and the decrease in inter-sandwich S-3p/S-3p interaction, as a result of intercalation.

Furthermore, the effect of the strong deformation of the TiS_2 slabs at the transition from $NaTiS_2$(I) to $NaTiS_2$(II) (c-axis contraction and a-axis elongation) on the band structure is calculated. The flattening of the slabs brings on an increased Ti–S ionicity, which manifests itself in an increase of the Ti-3d/S-3p gap, a narrowing of the conduction bands and a larger value of $N(E_F)$. These effects add to the increased ionicity due to the different coordination of the Na atoms and the concomitant different stacking of the slabs.

From the band-structure calculations for TiS_2, $LiTiS_2$, $NaTiS_2$(I) and $NaTiS_2$(II) we deduced values for inter-sandwich and intra-sandwich interactions between S $3p_z$ orbitals. These interactions show a clear relation with inter-sandwich and intra-sandwich distances. The intra-sandwich interaction is strongest for the $NaTiS_2$(II) structure, with the flattened TiS_2 sandwiches.

The Fermi surface changes from a single electron sheet in $NaTiS_2$(I) to a Fermi surface, consisting of two sheets in $NaTiS_2$(II), one with electron-like and one with hole-like character.

The band structure of $AgTiS_2$ shows clearly the effect of the Ag 4d states on the bonding.

Acknowledgment

We gratefully acknowledge discussions with Dr R A de Groot and Dr H J M Bouwmeester.

References

Ahmad N, Klipstein P C, Obertelli S D, Marseglia E A and Friend R H 1987 *J. Phys. C: Solid State Phys.* **20** 4105

Barry J J, Hughes H P, Klipstein P C and Friend R H 1983 *J. Phys. C: Solid State Phys.* **16** 393

Bouwmeester H J M 1988 *PhD Thesis* Groningen

Chianelli R R, Scanlon J C and Thomas A H 1975 *Mater. Res. Bull.* **10** 1379

Coehoorn R, van Heuzen A A, Haas C and Sawatzky G A 1985 *Festkörperprobleme (Advances in Solid State Physics)* vol 25 (Braunschweig: Vieweg) p 459

Dahn J R, McKinnon W R, Haering R R, Buyers W J M and Powell B M 1980 *Can. J. Phys.* **58** 207

Dijkstra J 1987 unpublished results

Doni E and Girlanda R 1986 *Electronic Structure and Electronic Transitions in Layered Materials* ed. V Grasso (Dordrecht: Reidel) p 1

Gerards A G 1987 *PhD Thesis* Groningen University

Gerards A G, Roede H, Haange R J, Boukamp B J and Wiegers G A 1984/1985 *Synth. Met.* **10** 51
Hibma T 1980 *J. Solid State Chem.* **34** 97
—— 1982 *Intercalation Chemistry* ed. M Whittingham and A J Jacobsen (New York: Academic) p 285
Huisman R, de Jonge R, Haas C and Jellinek F 1971 *J. Solid State Chem.* **3** 56
Inoue M, Matsumoto M, Negishi H and Sakai H 1985 *J. Magn. Magn. Mater.* **53** 131
Klipstein P C and Friend R H 1987 *J. Phys. C: Solid State Phys.* **20** 4169
Koyano M, Negishi H, Ueda Y, Sasaki M and Inoue M 1986 *Phys. Status Solidi* b **138** 357
—— 1987 *Solid State Commun.* **62** 261
Mattheiss L F 1973 *Phys. Rev.* B **8** 3719
McCanny J V 1979 *J. Phys. C: Solid State Phys.* **12** 3263
Meakin J I, Klipstein P C and Friend R H 1987 *J. Phys. C: Solid State Phys.* **20** 271
Methfessel M and Kübler J 1982 *J. Phys. F: Met. Phys.* **12** 141
Molinie P, Trichet L, Rouxel J, Berthier C, Chabre Y and Segransan P 1984 *J. Phys. Chem. Solids* **45** 105
Mori M, Ohshima K, Moss S C, Frindt R F, Plichke M and Irvin J C 1982 *Solid State Commun.* **43** 781
Myron H W 1980 *Physica* B **99** 243
Myron H W and Freeman A J 1975 *Phys. Rev.* B **11** 2735
Negishi H, Shoube A, Takahashi H, Ueda Y, Sasaki M and Inoue M 1987 *J. Magn. Magn. Mater.* **67** 179
Onuki Y, Inada R, Tanuma S, Yamanaka S and Kamimura H 1982 *J. Phys. Soc. Japan* **51** 880
Rouxel J 1976 *J. Solid State Chem.* **17** 223
—— 1979 *Intercalated Layered Materials; Physics and Chemistry of Layered Materials* vol 6 ed. F Levy (Dordrecht: Reidel) p 201
Starnberg H I and Hughes H P 1987 *J. Phys. C: Solid State Phys.* **20** 4429
Umrigar C, Ellis D E, Ding-sheng Wang, Krakauer H and Posternak M 1982 *Phys. Rev.* B **26** 4935
Van Bruggen C F 1982 *Ann. Chim. Fr.* 7 171
Whangbo M H, Rouxel J and Trichet L 1985 *Inorg. Chem.* **24** 1824
Whittingham M S 1978 *Prog. Solid State Chem.* **12** 41
Wiegers G A 1980 *Physica* B **99** 151
Wiegers G A, Bronsema K D, van Smaalen S, Haange R J, Zondag J E and de Boer J L 1987 *J. Solid State Chem.* **67** 9
Williams A R, Kübler J and Gelatt C D Jr 1979 *Phys. Rev.* B **19** 6094
Wilson J A 1977 *Solid State Commun.* **22** 551
Yamasaki T, Suzuki N and Motizuki K 1987 *J. Phys. C: Solid State Phys.* **20** 395
Zunger A and Freeman A J 1977 *Phys. Rev.* B **16** 906